International Journal of Sustainable and Green Energy
2019; 8(3): 56-64
http://www.sciencepublishinggroup.com/j/ijsge
doi: 10.11648/j.ijrse.20190803.12
ISSN: 2575-2189 (Print); ISSN: 2575-1549 (Online)

Consideration of Double Discrete Inclined Ribs in Low Curvature Coil for GSHP System

Teguh Hady Ariwibowo[1, 2, *], Akio Miyara[3, 4], Keishi Kariya[3]

[1]Graduate School of Science and Engineering, Saga University, Saga, Japan

[2]Department of Power Plant Technology, Politeknik Elektronika Negeri Surabaya (PENS), Surabaya, Indonesia

[3]Department of Mechanical Engineering, Saga University, Saga, Japan

[4]International Institute of Carbon-Neutral Energy Research, Kyushu University, Fukuoka-shi, Japan

Email address:

teguhhady@pens.ac.id (T. H. Ariwibowo), miyara@me.saga-u.ac.jp (A. Miyara), kariya@me.saga-u.ac.jp (K. Kariya)

[*]Corresponding author

To cite this article:

Teguh Hady Ariwibowo, Akio Miyara, Keishi Kariya. Consideration of Double Discrete Inclined Ribs in Low Curvature Coil for GSHP System. *International Journal of Sustainable and Green Energy.* Vol. 8, No. 3, 2019, pp. 56-64. doi: 10.11648/j.ijrse.20190803.12

Received: July 8, 2019; **Accepted**: August 6, 2019; **Published**: August 19, 2019

Abstract: This article presents an investigation of a low curvature coiled tube with double discrete inclined ribs for an application to ground heat exchanger used in ground heat pump systems. Computational fluid dynamics is employed to analyze the heat transfer and fluid flow with several ribs. The analysis performs detailed study involving flow behavior, pressure drop, heat transfer rate, wall heat flux, absolute vorticity flux for a range of ribs height (0.45 mm, 0.75 mm, and 1 mm) and flowrate (ranging from 6 L/min to 10 L/min) on curvature of coil 2.22 m^{-1}. COP improvement factor, which is a function of heat transfer enhancement and pressure loss increase, is evaluated. The increasing of ribs height can deviate secondary flow, which contributes to heat transfer and pressure drop enhancement. In the case of higher ribs, circumferential heat flux distribution tends to be more fluctuated. The heat flux distribution also becomes smaller with the increasing of axial distance. The COP improvement factor significantly improves with the increase of ribs height. On the other hand, the COP Improvement factor tends to decrease with the increase in flow rate. The application of ribs in a low curvature coil is attractive and has the potential for Slinky-coil ground heat exchangers.

Keywords: Double Discrete Inclined Ribs, Low Curvature Coil, Ground Source Heat Exchangers

1. Introduction

The increase in global warming has triggered a rise in the use of renewable energy sources. The Ground Source Heat Pump (GSHP) system is a technology which utilizes renewable energy. This system can improve the efficiency of cooling and heating in commercial buildings. GSHP is connected to Ground Heat Exchanger (GHE) with vertical or horizontal configurations. GHE is used to reject heat to the ground or to absorb heat from the ground. Vertical configurations are usually installed at depths from 15 to 150 m while horizontal configuration can be installed in trenches with depths from 1 to 2 m.

One of GHE horizontal configuration is slinky. The slinky GHE has better thermal performance compared to straight pipes [1-4]. The slinky pipe curvature is capable of producing secondary flow resulting from centrifugal force. The amount of research on slinky-coil GHE is not as much as research on GHE straight pipes. The use of two GHE slinky-coil sets in a long time and the number of different loop angles compared to the heat transfer capability has been investigated by Fujii et al. [5]. However, the complexity of the slinky-coil, mathematical models have never been used to predict the performance of slinky GHE in a long time.

Several developments were made to improve the slinky performance of GHE. These include the vertical and horizontal configurations while geometry-based variations on coil pitch distance, coil diameter, tube diameter, tube material, the length between slinky and ground composition.

Chong et al. [6] researched the effect of slinky performance on numerical vertical and horizontal configurations. The results of this study indicate that both configurations produce differences in thermal performance with a maximum of less than 5%.

Ali et al. [7] researched slinky in experimental vertical and horizontal configurations. They stated that vertical configuration tends to perform more superior than horizontal configuration on the heat extraction rate. Wanda et al. [8] observed the effect of the number of loops, tube material, and the distance between loops. They stated that the operation of the double and triple loops produced higher thermal performance 83% and 162%, respectively, compared to one loop at the same pump power. The use of copper pipes results in an average heat transfer increase of 48% compared to HDPE pipes. In parallel operations, thermal performance can increase from 10% to 14% when there were distances between loops available. Mostly slinky GHE is low curvature coil. Hardik et al. [9] researched several curvatures of the coil. They concluded that large curvature has high heat transfer. Strong secondary flow contributes to high heat transfer.

Some researchers observed the flow pattern of the coil pipe. Some articles depict hydrodynamic characters such as velocity fields, secondary flow, and pressure drop in theory [10-12], experiments [13-14], or numeric [15-16]. Some process parameters are examined with several different boundary conditions, such as constant heat flux, constant temperature, or convection heat transfer [17-19].

Wang and Sunden [20] studied the heat transfer and flow of fluid in a square channel with broken V-shape ribs using the LCT and PIV techniques. They concluded that broken ribs had better performance at high Reynolds numbers. Meng et al. [21] found that the use of the discrete double inclined rib tube (DDIR-tube) generates multiple vortexes on the laminar flow so that heat transfer increases. Li et al. [22] inject ink to see flow patterns inside the DDIR-tube. Tang et al. [23] observed the flow structure and heat transfer in the rectangular pipe with the addition of discrete rib arrays using numerical simulations and experiments. Kathait and Patil [24] conducted experiments on heat transfer and friction factors of a corrugated tube with gaps. Zheng et al. [25] investigated DDIR-tube effect of three pairs of v-type ribs by using numerical simulation. They concluded that ribs could produce three pairs of counter-rotating vortex and mainstream flow divided into six helical streams. This flow makes the intense turbulent mixing between the wall and the core of the flow.

As far as the author's knowledge, no research has been carried out in the modeling of modified coil pipe shapes to improve GHE performance. The purpose of our study is to overcome low curvature coil by adding DDIR on the coil wall. This research is to clarify the impact of DDIR use on improving the performance of heat transfer and fluid flow for ground-source heat pump system applications.

2. Simulation of DDIR in Low Curvature Coil

2.1. Model Description

As shown in Figure 1 (a)-(d), the tube is divided into three parts, namely the entrance, ribbed coil, and exit region. Entrance and exit regions have a length (l) of 200 mm while the axial length of the ribbed coil section is 3.53 m. The inner diameter of the tube (d) is 14.46 mm tube thickness is 0.71 mm, coil pitch (P) is 100 mm, coil diameter (D) is 900 mm (curvature of coil 2.22 m^{-1}), the double discrete inclined ribs details are ribs pitch (p) is 22 mm, then number of circumference of ribs was 4, inclination angle of ribs is (α) 45°, three values height of ribs 0.45 mm (RHC1), 0.75 mm (RHC2) and 1 mm (RHC3), were used to investigate on thermo-hydraulic performance on coil ribbed tube. Coil plain tube (PC) was used to see improved performance of the DDIR.

2.2. Numerical Method

Numerical simulations were carried out by utilizing commercial CFD software, ANSYS FLUENT 17.2, to examine the ribbed coil.

The governing equations of flow and heat transfer inside the tube are as follows [26]:

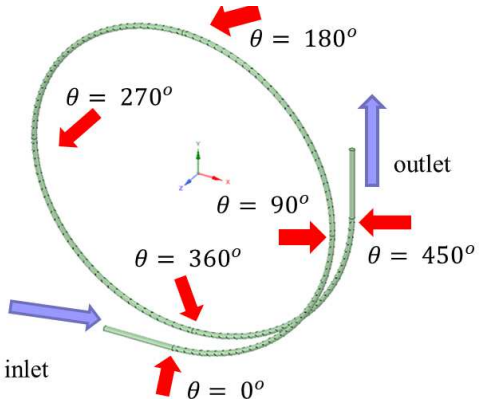

(a)

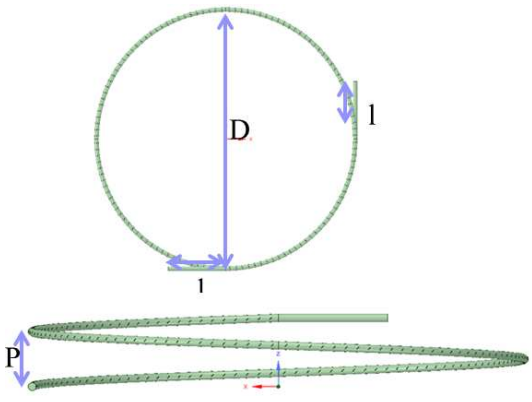

(b)

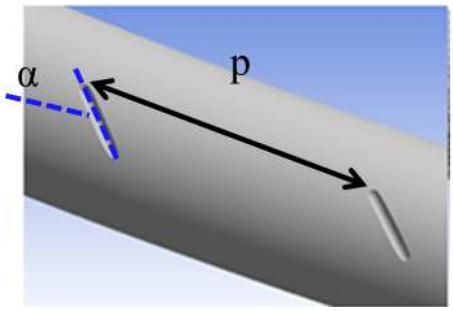

(c)

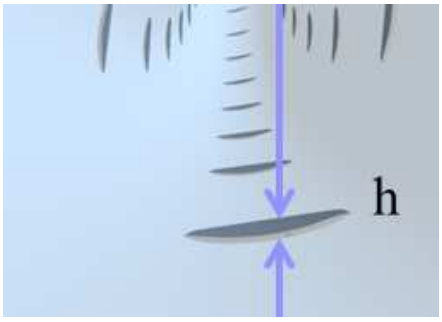

(d)

Figure 1. *(a) General view of the computational domain and several cross-sections of the coil for data collection; (b) view from top and side; (c) Location of ribs outside view; (d) Location of ribs inside.*

Continuity Equation:

$$\frac{\partial(\rho \mathrm{u}_i)}{\partial x_i}=0 \tag{1}$$

Momentum Equation:

$$\frac{\partial(\rho \mathrm{u}_i)}{\partial t}+\frac{\partial(\rho \mathrm{u}_i \mathrm{u}_j)}{\partial x_j}=-\frac{\partial p}{\partial x_i}+\frac{\partial}{\partial x_j}\left(\mu\frac{\partial(\mathrm{u}_i)}{\partial x_j}-\rho\overline{u_i' u_j'}\right) \tag{2}$$

Energy Equation:

$$\frac{\partial(\rho T)}{\partial x_i}+\frac{\partial(\rho \mathrm{u}_i T)}{\partial x_i}=\frac{\partial}{\partial x_i}\left(\frac{\lambda}{c_p}\frac{\partial T}{\partial x_i}\right) \tag{3}$$

Turbulence Kinetic Energy Equation:

$$\frac{\partial(\rho T)}{\partial x_i}+\frac{\partial(\rho \mathrm{u}_i T)}{\partial x_i}=\frac{\partial}{\partial x_i}\left(\frac{\lambda}{c_p}\frac{\partial T}{\partial x_i}\right) \tag{4}$$

Where ρ, T, λ and c_p are density, temperature, thermal conductivity, and heat capacity specific, respectively.

The boundary conditions used in this simulation are as follows. On the inlet side, uniform velocity is used, while the outflow boundary condition is used on the outlet side. Assumption of non-slip and uniform wall temperature conditions on the wall and ribs are used. Water is selected as a working fluid. All simulations use the steady flow approach with Reynolds numbers from 6172 to 10288. The SIMPLE algorithm is used for velocity-pressure coupling. Discretization of the governing equation utilizes the second-order upwind scheme. The minimum convergence criterion was 10^{-3} for continuity, velocity and turbulence equations and 10^{-7} for energy equation.

2.3. Data Reduction

Based on the simulation results of velocity and temperature filed, the average heat transfer coefficient can be determined by applying logarithmic mean temperature difference (LMTD) on heat transfer rate where:

$$Q=\dot{m}c_p(T_o-T_i) \tag{5}$$

$$h=\frac{Q}{\int_A dA\,\Delta T_m} \tag{6}$$

Where LMTD can be written as follows

$$\Delta T_m=\frac{(T_w-T_o)-(T_w-T_i)}{\ln\left(\frac{T_w-T_o}{T_w-T_i}\right)} \tag{7}$$

Where m, T_o, T_i, T_w and c_p are is mass flowrate, the bulk temperature at upstream, downstream and wall of the coil, and specific heat capacity, respectively. The use of LMTD is valid because based on the assumption, the property value of the working fluid is constant. Wall temperature is set as same as ground Temperature on our previous research [7].

Reynolds number, Nusselt number, friction factors are determined as follows:

$$\mathrm{Re}=\frac{\rho u d}{\mu} \tag{8}$$

$$Nu=\frac{hD}{\lambda} \tag{9}$$

$$f=\frac{\Delta p}{(l/d)\left(\rho\frac{v^2}{2}\right)} \tag{10}$$

Where μ, h, and l are dynamics viscosity, heat transfer coefficient, axial length tube.

Ito's Critical Reynolds number is used to calculate the transition from laminar to turbulent flow.

$$\mathrm{Re}_{cr}=20000\left(\frac{d}{D}\right)^{0.32} \tag{11}$$

DDIR of the coil is evaluated by the Coefficient of Performance (COP) improvement factor that has been developed by Jalaluddin and Miyara [27] in equation 12.

$$\frac{Q_H'}{Q_H}-\frac{V\Delta p}{Q_H}\frac{\Delta p'}{\Delta p}>0 \tag{12}$$

where Q_H , $Q_H^{'}$, V, $\Delta p^{'}$, Δp are heating rate (W/m), an increase of heating rate (W/m), volumetric flow rate (m^3/s), an increase of pressure drop (Pa), and pressure drop (Pa), respectively.

All of the COP improvement factors are evaluated based on heat transfer and fluid flow of straight tube by using Nusselt number and friction factor in a smooth straight tube.

2.4. Mesh Elements Independence Test

Ansys Meshing 17.2 is used to produce three-dimensional meshing. Fluid domains are discretized using unstructured mesh elements. The mesh distance near the tube and ribs wall is calculated based on $y^+ = 1$ to produce a more accurate result.

Table 1. *Grid Independence Test.*

GHE Type	Coarse	Medium	Fine[+]
DDIR Coil (Number of Elements)	18168327	181645194	19008154
Pressure Drop (Pa/m)	589.471	592.568	592.929
Relative Deviation	0.077%	0.060%	-
Heat Transfer Coefficient (W/(m^2K))	3172.4	3169.6	3172.15
Relative Deviation	0.007 %	0.080%	-

[+] Fine mesh results are selected as the base of relative deviation.

3. Results and Discussion

To give a good explanation of the thermo-hydraulic effect DDIR on coil tube, we investigate temperature and velocity contour, circumferential heat flux, and vortex intensity.

3.1. Model Validation

The simulation results were compared with the Gnielinski correlation for the Nusselt number and Petukhov correlation for friction factors in the turbulent flow through smooth pipe To verify the accuracy of the numerical simulation procedures applied in this research.

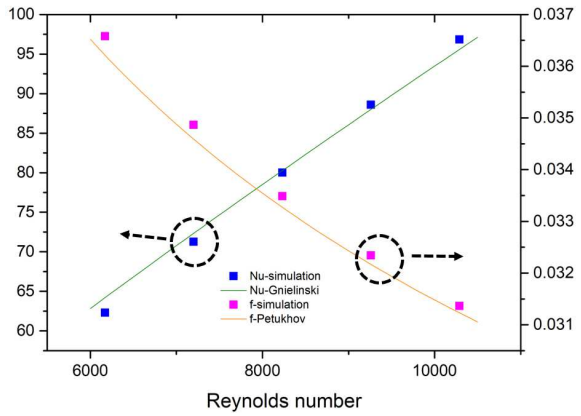

Figure 2. *Validation of smooth tube friction factor and Nusselt number.*

Figure 2 illustrates the comparison between simulation results and correlation. The simulation results confirm the correlations within 1% and 7.6% for friction factor and Nusselt number, respectively.

3.2. Fluid Flow Characteristics

In this analysis, cold water at 280 K with a Re = 8230 enters the helical pipe with a predetermined boundary condition. The working fluid is made to heat up when it flows along with the coil with a wall temperature of 291 K. The critical Re in the coil is 5332. The turbulent intensity is calculated based on the empirical correlation for pipe flows as follows [26].

$$I = 0.16\left(\mathrm{Re}_{D_H}\right)^{-1/8} \tag{13}$$

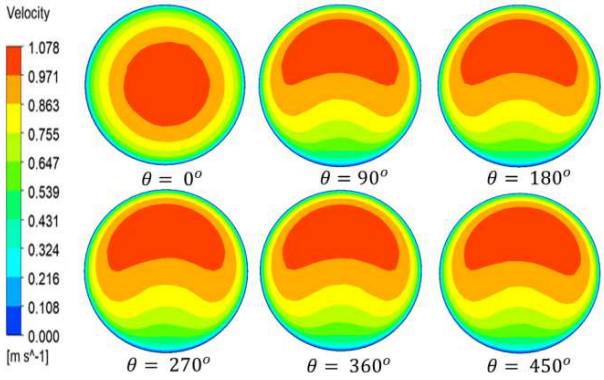

(a)

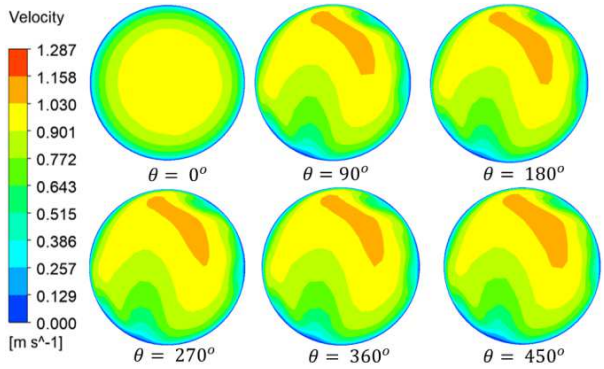

(b)

Figure 3. *Evolution of velocity contour along the axial length of the coil at Re = 8230, top and downside of the tube are outer side and inner side of the coil (a) PC; (b) RHC2.*

Figure 3 shows the evolution of velocity contour in several axial positions along the length of the coil (every 90°, i.e., ¼ turns) from 0° to 450°. It can be seen that both PC and RHC2 have reached fully developed flow at first θ = 90°, the further velocity contours keep a constant shape. Both tubes also indicate the high velocity shifted from the center of the tube at θ= 0° to outside of the coil. This phenomenon is caused by the secondary flow of the coil. However, the velocity magnitude contour of the ribbed tube is somewhat distorted. It may be caused by flow by the ribs. Figure 4 shows the effect DDIR on pressure drop at various flow rates. An apparent trend is found where pressure drop increases with the increase of ribs height. PC and RHC1 have similar pressure drop values, especially at

a low flow rate when compared to RHC2 and RHC3. The RHC2 and RHC3 suffer more pressure drop than that of PC. Higher flow rate effect could be more domination in this phenomenon, although the higher flowrate leads to smaller friction factors in all tubes. The pressure drop could be triggered by ribs generated flow generated. The maximum frictional pressure drop of RHC3 is about 124% greater than that of PC at V = 10 L/m.

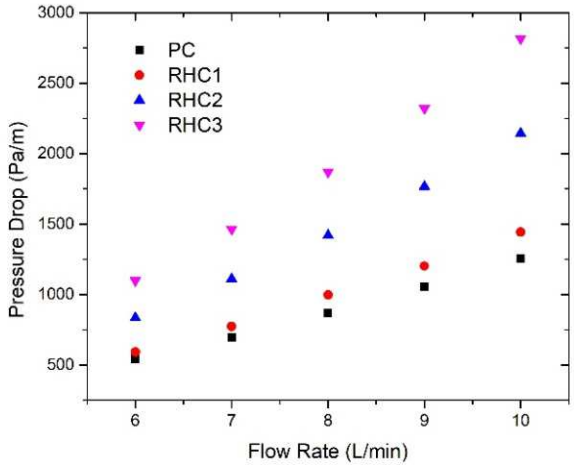

Figure 4. *Comparison of pressure drop in different configuration of ribs.*

3.3. Heat Transfer Characteristics

The thermal performance of DDIR in the coil was studied concerning heat transfer rate and temperature distribution within several cross-sections of the tube. Figure 5 shows the effect of flow rate on the heat transfer rate for PC and RHC. It can be seen that heat transfer rate almost linearly increases with an increase in flowrate for curved tube ribs as well as curved tube plain. However, the amplitude of variation of all variation of RHC is more significant than that of for PC, which can attribute to the better mixing caused by longitudinal swirls flow in the ribs. The highest heat transfer rate is obtained by RHC3, which relatively larger about 27 % greater than that of PC at V = 10 L/m.

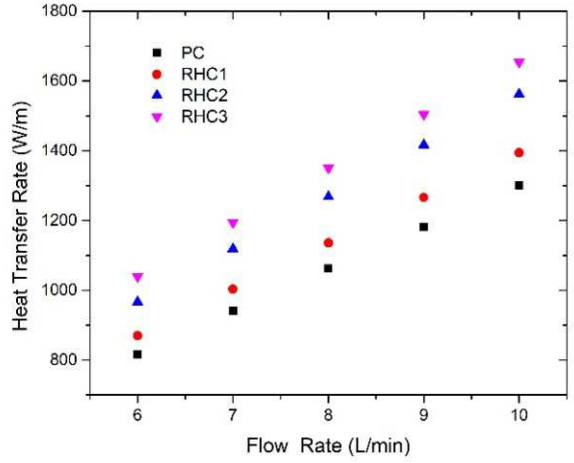

Figure 5. *Comparison of heat transfer rate in different configuration of ribs.*

Figure 6, It can be seen that longer axial distance or more significant coil angle tend to have more uniformity temperature profile. The colder fluid in the core of the tube at θ= 0^o tends to move to the outer side of the coil at θ= 90^o on both tubes by increasing coil angle. However, the temperature profile of the ribbed tube is somewhat distorted. The temperature profile of curved tube ribs looks hotter compared to the curved tube plain at the same position above θ= 90^o. It could be caused by thermal mixing of flow generated by the ribs.

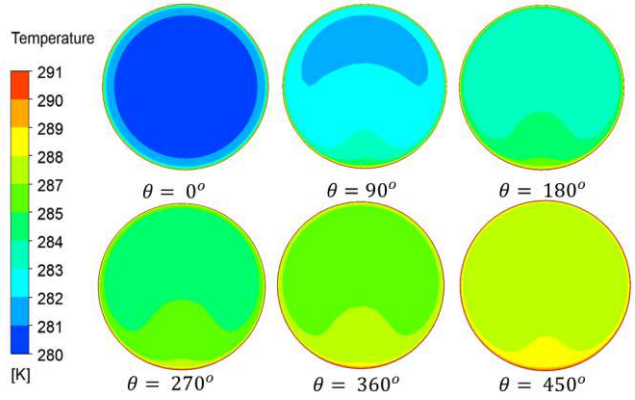

(a)

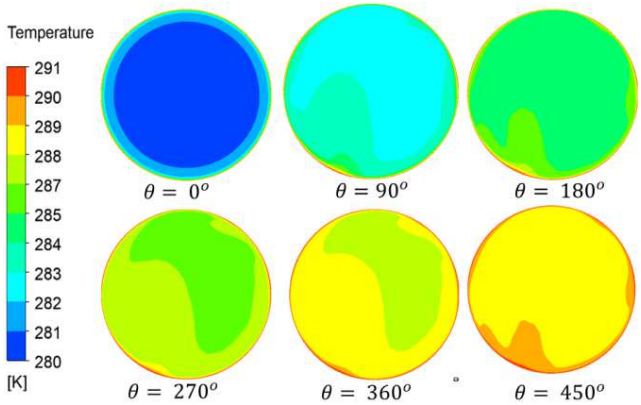

(b)

Figure 6. *Evolution of temperature contour along axial length of the coil at Re = 8230, top and downside of the tube are outside and inner side of coil (a) PC; (b) RHC2.*

3.4. Wall Heat Flux

Figure 7 shows the circumferential distribution (β) of heat flux surfaces calculated from the local wall temperature, local bulk temperature, and fluid-side local heat transfer coefficient. The overview of this distribution of Figure 8(a) is following the Xin and Ebidian [28] and Hardik et al. [9] studies on the plain coil. Surface heat fluxes have varying sinusoidal values in the circumferential direction. Heat flux distribution is a mirror of the temperature difference distribution between the wall and fluid near the wall. Therefore, a small difference from the difference in temperature between fluids near walls and walls can result in significant changes to the surface heat flux.

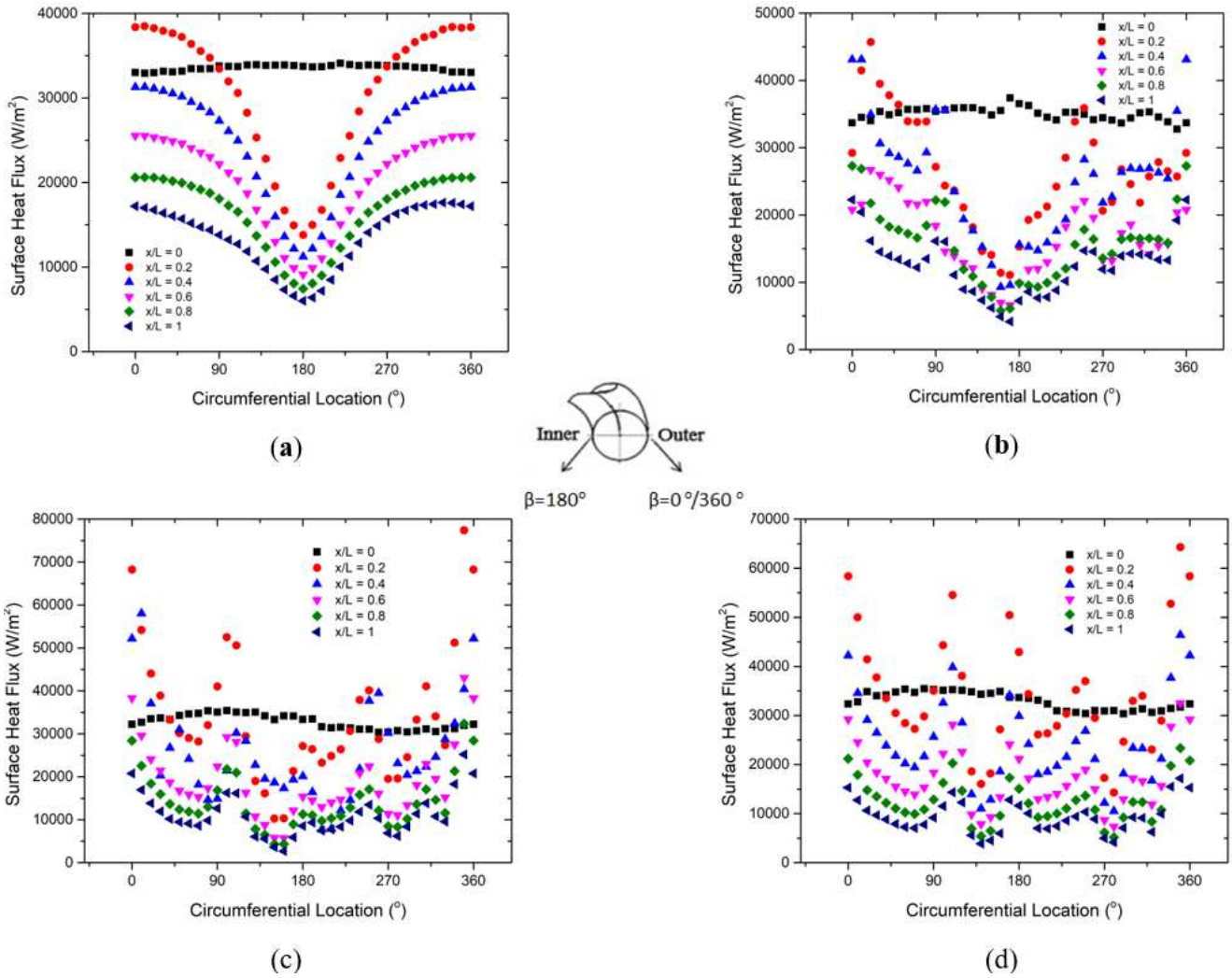

Figure 7. *Circumferential surface heat flux distribution at different axial point of coil at Re = 8230 (a) PC; (b) RHC1; (c) RHC2; (d) RHC3.*

On the outside and inside of the coil, the surface of the heat flux is sinusoidal. Surface heat transfer is the maximum value on the outermost side at 0^o or 360^o, while the minimum value is on the inner side at 180^o.

In Figure 7 (b)-(d), all RHC variations have higher fluctuation of wall heat flux than that of PC. The higher height of ribs can contribute to the more considerable change of wall heat flux distribution. Generally, the increment of the height of ribs indicates lower wall heat flux at each axial location. This trend shows decrement in heat transfer caused by the bulk temperature approaching wall temperature. It can be seen that there are significantly bottomed out of surface heat fluxes in several circumferential locations. The distribution pattern could be contributed by proper thermal mixing due to the flow generated by the ribs.

3.5. Secondary Flow Pattern

Figure 8 illustrates the variation of the vortex location for different ribs at the same Reynolds number. Based on Zheng et al. [25] research, the use of double discrete inclined ribs (DDIR) on straight pipes can generate several vortices. However, in our research, we did not find any additional vortexes in ribs application on low curvature coil. In general view, vortex deflection has increased with increasing size of ribs, streamlined changing from smooth pattern to distorted pattern. The distorted pattern could be resulted by the merge of the main flow and DDIR's induced flow. Based on the above analysis at the same Reynolds number, vortex deflection will increase with increasing height of ribs, and pressure loss will be more significant and more distorted vortex deflection conditions than the smaller ribs. The more distorted vortex could contribute to enhanced heat transfer.

To find out the influence of secondary flow in this study, our research use method, which was proposed by Lin et al. [29] and Tang et al. [30]. They apply absolute vorticity flux intensity to relate improvement of heat transfer and pressure drop on the pipe. The intensity can illustrate the flow field in the coil. This parameter is a crucial factor for secondary flow typical features. It can be described as eq (14)

$$J_{ABS}^{n} = \frac{1}{A}\iint \left|\omega^{n}\right| dA \tag{14}$$

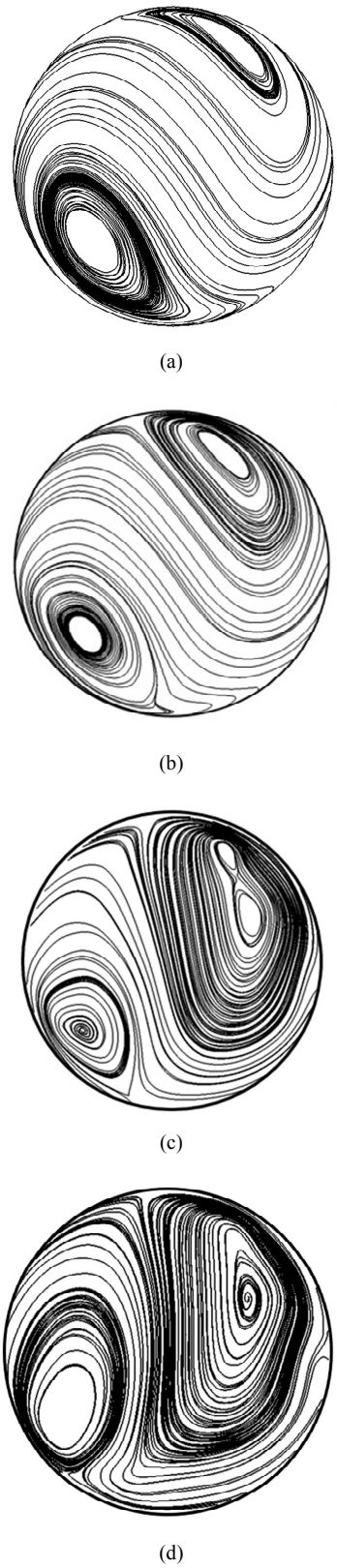

(a) (b) (c) (d)

Figure 8. *Secondary flow in Re = 8230 top and downside of tube are outer side and inner side of coil, respectively (a) PC; (b) RHC1; (c) RHC2; (d) RHC3.*

Where A, n, and ω are cross-section area (m^2), the direction of the normal cross-section and vorticity, respectively. Vorticity is a curl of u-velocity in the flow field. The vorticity can be stated as follows

$$\omega = \nabla \times u \tag{15}$$

Figure 9 shows changes in absolute vorticity flux. Secondary flow intensity gradually increases with increasing flow rate, which occurs both at curved tube plain and curved tube ribs. RHC1 tend to perform slightly better than the PC on the same flow rate. What is interesting in this graph is the dramatic increase in vortex intensity in RHC2 and RHC3. This phenomenon could be affected by the significant deviation of secondary flow, as shown in Fig 8. The characteristics of absolute vorticity flux could be the reason why pressure drop and heat transfer, in Figure 4 and 5, PC and RHC1 have almost similar value meanwhile RHC2 and RHC3 tends to have higher pressure drop and heat transfer than PC.

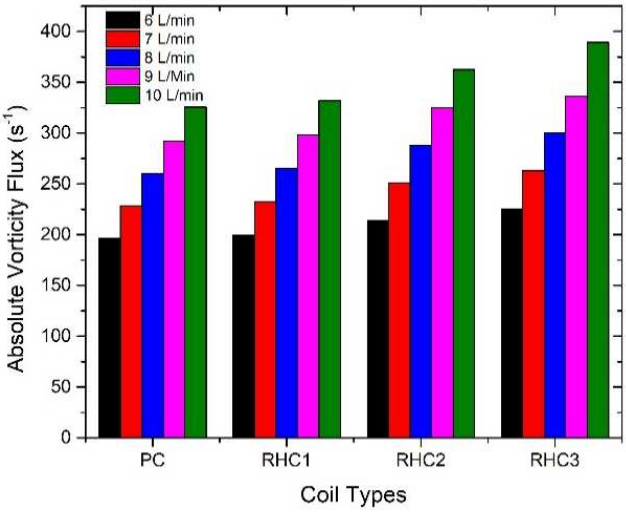

Figure 9. *Variation of absolute vorticity flux with type of coil and flow rates.*

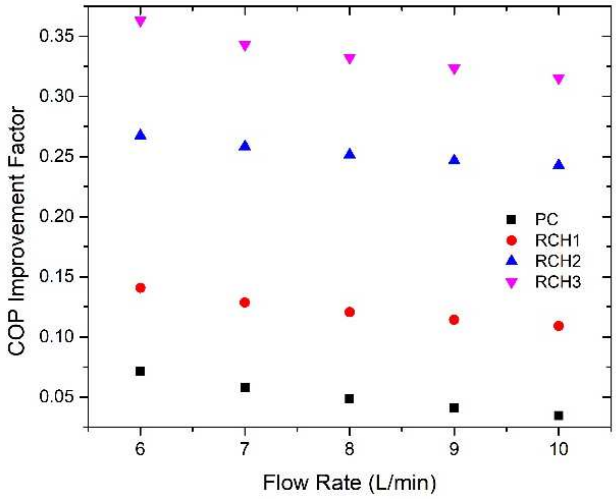

Figure 10. *Effect of double discrete inclined ribs on COP Improvement factor at various flowrates.*

Generally, COP improvement factors, as shown in Figure 10 are always positive. The use of higher ribs results in a COP Improvement factor that is very significant compared to the

plain coil. However, the increase in flowrate decreases the COP improvement factor slowly. This could be caused by an increase in energy from the use of ribs compensated with energy loss due to pressure drop. The rate of this COP Improvement factor will probably level off at higher flow rate.

4. Conclusion

The results of numerical study of heat transfer and pressure drop enhancement in DDIR applied to low curvature coil are described in this paper. Based on the result, the following conclusions are drawn.

1. Pressure drop and heat transfer dependent on ribs height of low curvature coil.
2. Circumferential wall heat flux on PC is varying sinusoidal form. Meanwhile, the heat flux distributions of RHC tend to fluctuate. Higher ribs contribute higher fluctuation of heat flux. The longer axial distance contributes to the lower heat flux due to the bulk temperature approaching to wall temperature.
3. The usage of higher ribs could contribute a higher deviation vortex than that of PC.
4. The characteristics of pressure drop and heat transfer could be related to the absolute vorticity flux.
5. The higher ribs can enhance COP improvement factor. Maximum improvement at given flow rate COP is RHC3 eightfold higher than PC. However, increasing flowrate tends to decrease COP Improvement factors.

Acknowledgements

This research was supported by the "Renewable energy heat utilization technology and development project" of the New Energy and Industrial Technology Development Organization (NEDO), Japan.

References

[1] D. Adamovsky, P. Neuberger, R. Adamovsky, “Changes in energy and temperature in the ground mass with horizontal heat exchangers—The energy source for heat pumps”. Energy and Buildings, 2015, Vol. 92, pp. 107-115.

[2] S, Yoon, S. R. Lee, H. G. Go, “Numerical modeling of slinky-coil horizontal ground heat exchangers. Energy and Buildings”, 2015, Vol. 105, pp. 100-105.

[3] P. M. Congedo, G. Colangelo, G. Starace, “CFD simulations of horizontal ground heat exchangers: a comparison among different configurations”. Applied Thermal Engineering, 2012, vol. 33-34, pp. 24-32.

[4] Y. Wu, G. Gan, A. Verhoef, P. L. Vidale, R. G. Gonzalez, “Experimental measurement and numerical simulation of horizontal-coupled slinky ground source heat exchangers”, Applied Thermal Engineering, 2010, vol. 30, pp. 2574-2583.

[5] H. Fujii, K. Nishi, Y. Komaniwa, N. Chou, “Numerical modeling of slinky-coil horizontal ground heat exchangers”. Geothermics, 2012, vol. 41, pp. 55-62.

[6] Y. Chong, G. Gan, A. Verhoef, R. G. Garcia, “Comparing the thermal performance of horizontal slinky-loop and vertical slinky-loop heat exchangers”. International Journal of Carbon Technology, 2013, vol. 9, pp. 250–255.

[7] M. H. Ali, K. Kariya, A. Miyara, “Performance Analysis of Slinky Horizontal Ground Heat Exchangers for a Ground Source Heat Pump System”. Resources, 2017, vol. 6, pp. 1-18.

[8] Wanda, S.; Miyara, A.; Kariya, K. Analysis of Short Time Period of Operation of Horizontal Ground Heat Exchangers. Resources. 2015, 4, 507-523.

[9] B. K. Hardik, P. K. Baburajan, S. V. Prabhu, “Local heat transfer coefficient in helical coils with single phase flow”. International Journal of Heat and Mass Transfer, 2015, vol. 89, pp. 522-538.

[10] W. R. Dean, “Note on the motion of fluid in a curved pipe”. The London, Edinburgh, and Dublin Philosophical Magazine and Journal of Science 1927, vol. 4, pp. 208-223.

[11] W. R. Dean, “The stream-line motion of fluid in a curved pipe”, The London, Edinburgh, and Dublin Philosophical Magazine and Journal of Science, 1928, vol. 5, pp. 673-695.

[12] S. Agrawal, G. Jayaraman, V. K. Srivastava, K. D. P. Nigam, “Power law fluids in a circular curved tube. Part I. Laminar flow”. Polymer-Plastics Technology and Engineering, 1993, vol. 32, pp. 595-614.

[13] L. R. Austin, J. D. Seader, “Entry region for steady viscous flow in coiled circular pipes”. American Institute of Chemical Engineers Journal, 1974, vol. 20, pp. 820-822.

[14] H. Saffari, R. Moosavi, M. N. Nouri, C. X. Lin, “Prediction of hydrodynamic entrance length for single and two-phase flow in helical coils”. Chemical Engineering and Processing: Process Intensification, 2014, vol. 86, pp 9-21.

[15] S. C. R. Dennis, M. Ng, “Dual solutions for steady laminar flow through a curved tube”. The Quarterly Journal of Mechanics and Applied Mathematics, 2010, vol. 30, pp. 305-324.

[16] S. Agrawal, K. D. P. Nigam, “Modelling of a coiled tubular chemical reactor”. Chemical Engineering Journal, 2001, vol. 84, pp. 437-444.

[17] D. G. Prabhanjan, T. J. Rennie, G. S. V. Raghavan, “Natural convection heat transfer from helical coiled tubes”. International Journal of Thermal Sciences, 2004, vol. 43, pp. 359-365.

[18] M. R. Salimpour, “Heat transfer coefficients of shell and coiled tube heat exchangers”, Experimental Thermal and Fluid Science. 2009, vol. 33, pp. 203-207.

[19] N. Jamshidi, M. Farhadi, D. D. Ganji, K. Sedighi, “Experimental analysis of heat transfer enhancement in shell and helical tube heat exchangers”. Applied Thermal Engineering, 2013, vol. 51, pp. 644-652.

[20] L. Wang, B. Sunden, “An experimental investigation of heat transfer and fluid flow in a rectangular duct with broken V-shaped ribs”, Experimental Heat Transfer. 2004, vol. 17, pp. 243-259.

[21] J. A Meng, X. G. Liang, Z. X. Li, “Field synergy optimization and enhanced heat transfer by multi-longitudinal vortexes flow in tube”. International Journal of Heat and Mass Transfer, 2005, vol. 48, pp. 3331-3337.

[22] X. W. Li, H. Yan, J. A. Meng, Z. X. Li, "Visualization of longitudinal vortex flow in an enhanced heat transfer tube". Experimental Thermal and Fluid Science, 2007, vol. 31, pp. 601-608.

[23] X. Y. Tang, D. S. Zhu, "Flow structure and heat transfer in a narrow rectangular channel with different discrete rib arrays". Chemical Engineering and Processing: Process Intensification, 2013, vol. 69, pp. 1-14.

[24] P. S. Kathait, A. K. Patil, "Thermo-hydraulic performance of a heat exchanger tube with discrete corrugations", Applied Thermal Engineering, 2014, vol. 66, pp. 162-170.

[25] N. Zheng, W. Liu, Z. Liu, P. Liu, F. A. Shan, "A numerical study on heat transfer enhancement and the flow structure in a heat exchanger tube with discrete double inclined ribs". Applied Thermal Engineering, 2015, vol. 90, pp. 232-241.

[26] ANSYS® Academic Research, Release 17.2, Help System, Fluent Theory Guide, ANSYS, Inc.

[27] Jalaluddin, A. Miyara, "Thermal performance and pressure drop of spiral-tube ground heat exchangers for ground-source heat pump". Applied Thermal Engineering, 2015, vol 9, pp. 630-637.

[28] R. C. Xin, M. A. Ebadian, "The effects of Prandtl numbers on local and average convective heat transfer characteristics in helical pipes", Journal of Heat Transfer, 1997, vol. 119, pp. 467-473.

[29] Z. M. Lin, L. D. Sun, L. B. Wang, "The relationship between absolute vorticity flux along the main flow and convection heat transfer in a tube inserting a twisted tape", Heat Mass Transfer, 2009, vol. 45, pp. 1351-1363.

[30] L. Tang, S. Yuan, M. Malin, S. Parameswaran, "Secondary vortex-based analysis of flow characteristics and pressure drop in helically coiled pipe", Advances in Mechanical Engineering, 2017, vol 9 (4), pp. 1-11.